Journal of Solid State Chemistry 184 (2011) 1517–1522

Contents lists available at ScienceDirect

Journal of Solid State Chemistry

journal homepage: www.elsevier.com/locate/jssc

$K_3Ln[OB(OH)_2]_2[HOPO_3]_2$ (Ln=Yb, Lu): Layered rare-earth dihydrogen borate monohydrogen phosphates

Yan Zhou [a,b], Stefan Hoffmann [a], Ya-Xi Huang [b], Yurii Prots [a], Walter Schnelle [a], Prashanth W. Menezes [a], Wilder Carrillo-Cabrera [a], Jörg Sichelschmidt [a], Jin-Xiao Mi [b], Rüdiger Kniep [a,*]

[a] Max-Planck-Institut für Chemische Physik fester Stoffe, Nöthnitzer Str. 40, 01187 Dresden, Germany
[b] Department of Materials Science and Engineering, College of Materials, Xiamen University, Xiamen 361005, PR China

ARTICLE INFO

Article history:
Received 13 December 2010
Received in revised form
7 April 2011
Accepted 10 April 2011
Available online 16 April 2011

Keywords:
Rare earth
Borate phosphate
Layered structure
Magnetic properties
EPR spectroscopy

ABSTRACT

Two isotypic layered rare-earth borate phosphates, $K_3Ln[OB(OH)_2]_2[HOPO_3]_2$ (Ln=Yb, Lu), were synthesized hydrothermally and the crystal structures were determined by single-crystal X-ray diffraction ($R\bar{3}$, Z=3, Yb: a=5.6809(2) Å, c=36.594(5) Å, V=1022.8(2) Å^3, Lu: a=5.6668(2) Å, c=36.692(2) Å, V=1020.4(1) Å^3). The crystal structure can be described in terms of stacking of Glaserite-type slabs consisting of LnO_6 octahedra interlinked by phosphate tetrahedra and additional layers of $[OB(OH)_2]^-$ separated by K^+ ions. Field and temperature dependent measurements of the magnetic susceptibility of the Yb-compound revealed Curie–Weiss paramagnetic behavior above 120 K (μ_{eff}=4.7 μ_B). Magnetic ordering was not observed down to 1.8 K.

1. Introduction

Recent research in the field of borophosphates has revealed that mild hydrothermal route is a promising synthetic approach in the exploration of the systems M_xO_y–B_2O_3–P_2O_5–(H_2O) (M=metal). This strategy has already resulted in numerous compounds with new crystal structures [1]. So far, this route of preparation was restricted to M representing main-group and/or transition elements. In contrast, our efforts are now focused on systems containing rare-earth elements. Up to now, the only reported examples for a rare-earth intermediates are given by the general formula $Ln_7O_6[BO_3][PO_4]_2$, (Ln=rare-earth element), prepared by solid state reaction at high temperatures [2].

Herein, we report on the synthesis and structure as well as physical characterization of two new hydrated rare-earth borate phosphates, which are obtained for the first time under mild hydrothermal synthesis conditions.

2. Experimental details

2.1. Hydrothermal synthesis

$K_3Yb[OB(OH)_2]_2[HOPO_3]_2$: Initially, 0.591 g Yb_2O_3 was dissolved in 1 mL concentrated HCl. Then, 1.8334 g $K_2B_4O_7 \cdot 4H_2O$, 3.658 g K_2HPO_4 and 4 mL H_2O (molar ratio of K:Yb:B:P=18:1:8:7) were mixed with the above solution, and the pH value was adjusted to 7 using 0.75 mL concentrated HCl. All starting materials used in the experiments were of analytical grade and were used without further purification. The mixture was transferred to a Teflon vessel with a cover, which was placed in a steel autoclave. The synthesis was conducted at 453 K for 5 days. After that time the autoclave was directly taken out of the hot oven. The product was filtered and washed with distilled water several times and dried at 323 K for 8 h. $K_3Lu[OB(OH)_2]_2[HOPO_3]_2$: 1.7340 g $LuCl_3 \cdot 6H_2O$, 1.8336 g $K_2B_4O_7 \cdot 4H_2O$ and 3.6372 g K_2HPO_4 were dissolved in 4 mL water and the pH value was adjusted to 6–7 using concentrated HCl. The suspension was transferred into a Teflon autoclave and maintained at 453 K for 3 days. Finally, the autoclave was directly taken out of the oven. Crystals settled at the bottom of the autoclave were washed with distilled water several times and dried at 323 K for 8 h.

2.2. Characterization

The chemical compositions of the products were determined using both inductively coupled plasma-optical emission spectrometry (ICP-OES) on a VARIAN Vista RL instrument and energy-dispersive X-ray spectroscopy (EDXS) carried out on a PHILIPS XL 30. ICP-OES results show that the molar ratio is K:Yb:B:P=2.45:1:1.47:1.78 (calc: 3:1:2:2) for $K_3Yb[OB(OH)_2]_2[HOPO_3]_2$, which suggests the presence of impurities not detected by powder X-ray diffraction (PXRD, Fig. S2). EDXS on three different crystals gave an average

* Corresponding author. Fax: +49 351 4646 3002.
E-mail address: kniep@cpfs.mpg.de (R. Kniep).

0022-4596/$ - see front matter © 2011 Elsevier Inc. All rights reserved.
doi:10.1016/j.jssc.2011.04.023

molar ratio of K:Yb:P=2.83:1:2.31. For $K_3Lu[OB(OH)_2]_2[HOPO_3]_2$ a molar ratio of K:Lu:B:P=2.95:1:1.93:1.97 is determined by ICP-OES, which is close to the ratio derived from single-crystal structure determination.

Thermal investigations (DTA/TG) were carried out in argon atmosphere with heating rates of 5 K/min up to 1273 K (NETZSCH STA 449). The FT-IR spectrum was recorded at room temperature using a Spectrum 100 Optical (PerkinElmer) with universal ATR sampling accessory. The magnetization measurements were performed on a SQUID-magnetometer (Quantum Design, MPMS XL-7) in the temperature range of 1.8–400 K using various external magnetic fields.

2.3. Crystal structure determination

Hexagonal platelets (Fig. S1) of the isotypic compounds $K_3Ln[OB(OH)_2]_2[HOPO_3]_2$ (*Ln*=Yb, Lu) were selected under a light microscope. Single-crystal X-ray diffraction data were collected on a Rigaku AFC7 (Mercury CCD detector) diffractometer using graphite-monochromated Mo *Kα* radiation (λ=0.71073 Å) at a temperature of 295 K. The isotypic structures were solved by direct methods and refined using the programs SHELXS-97 [3] and SHELXL-97 [3] included in the program suite WinGX [4]. The crystal structure of $K_3Lu[OB(OH)_2]_2[HOPO_3]_2$ was refined as a twin. The lattice parameters were determined by PXRD using LaB_6 as internal standard [5]. The final refinement by full-matrix least-squares methods led to: $K_3Yb[OB(OH)_2]_2[HOPO_3]_2$, M=603.95 g/mol, trigonal, $R\bar{3}$ (No. 148), a=5.6809(2) Å, c=36.594(5) Å, V=1022.8(2) Å^3, Z=3, 2119 measured and 757 independent reflections, $R1$=0.023 and $wR2$=0.054 for all data and $K_3Lu[OB(OH)_2]_2[HOPO_3]_2$, M=605.9 g/mol, trigonal, $R\bar{3}$, (No. 148), a=5.6668(2) Å, c=36.692(2) Å, V=1020.4(1) Å^3, Z=3, 3185 measured and 789 independent reflections, $R1$=0.027 and $wR2$=0.050 for all data. Further details are summarized in Table 1. Atomic positions and displacement parameters for $K_3Yb[OB(OH)_2]_2[HOPO_3]_2$ are given in Table 2. The crystallographic data were deposited at FIZ Karlsruhe under the CSD number 422902 ($K_3Yb[OB(OH)_2]_2[HOPO_3]_2$) and 422903 ($K_3Lu[OB(OH)_2]_2[HOPO_3]_2$).

3. Results and discussion

3.1. Crystal structure

Since both crystal structures are isostructural only the Yb-compound shown in Fig. 1 is discussed in detail. Ytterbium exhibits an octahedral coordination with a unique Yb–O distance of 2.202(2) Å (cf. selected bond lengths in Table 3) and two slightly different O–Yb–O angles of 88.2° and 91.8° (site symmetry C_{3i}). Phosphorous is in a distorted tetrahedral coordination of oxygen. Three corners of each tetrahedron are shared with three YbO_6 octahedra, and the corresponding P–O1 distances amount to 1.530(2) Å (3×, P site symmetry 3). A longer distance (1.551(4) Å) is observed for the remaining vertex (O2). These two types of polyhedra form a common 2D arrangement characteristic for the mineral Glaserite (Aphthitalite) [6], $K_3Na(SO_4)_2$. This structure type is adopted by a number of rare-earth compounds with the general formula $A_3Ln(XO_4)_2$ (*A*=Na, K, *Ln*=rare-earth element, *X*=P, V, As). The Glaserite-type layers can show different degrees of distortion [7]. The terminal P–O distance in the crystal structure of the Glaserite analog $K_3Lu(PO_4)_2$ [8] amounts to 1.505 Å and is shorter than the distance to the bridging oxygen atoms reflecting a general trend in the crystal chemistry of phosphates [9]. The three short O2···O3 distances

Table 2
Fractional atomic coordinates and equivalent displacement parameters (Å^2) for $K_3Yb[OB(OH)_2]_2[HOPO_3]_2$.

Atom	Wyckoff position	*x*	*y*	*z*	U_{eq}
Yb1	3*a*	0	0	0	0.011(1)
K1	3*b*	1/3	2/3	1/6	0.022(1)
K2	6*c*	1/3	2/3	0.0574 (1)	0.024(1)
P1	6*c*	2/3	1/3	0.0468(1)	0.010(1)
B1	6*c*	0	0	0.1159 (2)	0.018(1)
O1	18*f*	0.3713(4)	0.1840(5)	0.0336 (1)	0.019(1)
O2	6*c*	2/3	1/3	0.0891(1)	0.015(1)
O3	18*f*	0.2093(5)	0.2637(5)	0.1167 (1)	0.023(1)

Table 1
Crystal structure data and refinement parameters for $K_3Ln[OB(OH)_2]_2[HOPO_3]_2$ (*Ln*=Yb, Lu).

Empirical formula	$B_2\ K_3Yb\ O_{14}\ P_2\ H_6$	$B_2\ K_3\ Lu\ O_{14}\ P_2\ H_6$[a]
Formula weight (g/mol)	603.95	605.9
Temperature (K)	295	295
Crystal size (mm^3)	0.080×0.080×0.010	0.065×0.065×0.008
Radiation (Å)	Mo *Kα*, 0.71073	Mo *Kα*, 0.71073
Crystal system, space group	Trigonal, $R\bar{3}$ (No. 148)	Trigonal, $R\bar{3}$ (No. 148)
Unit cell parameters [b]	*a*=5.6809(2) Å	*a*=5.6668(2) Å
	c=36.594(5) Å	*c*=36.692(2) Å
	V=1022.8(2) Å^3	*V*=1020.4(1) Å^3
Z	3	3
Calculated density ρ_{calc} (g/cm^3)	2.942	2.958
Absorption coefficient μ (mm^{-1})	8.079	8.479
F(0 0 0)	855	858
θ range for data collection	3.34° to 32.08°	3.33° to 32.23°
Limiting indices	$-8 \le h \le 6, -4 \le k \le 6, -52 \le l \le 53$	$-6 \le h \le 8, -8 \le k \le 6, -52 \le l \le 52$
Reflections collected/unique	2119/757 [*R*(int)=0.0270]	3185/789 [*R*(int)=0.0373]
Goodness-of fit on F^2	1.067	1.076
$R1$,$wR2$ [$I>2\sigma(I)$]	0.0213, 0.0534	0.0238, 0.0497
$R1$,$wR2$ (all data)	0.0227, 0.0536	0.0267, 0.0504
Largest diff. peak and hole	0.838 and −1.412 e/Å^3	0.967 and −2.142 e/Å−3

[a] $K_3Lu[OB(OH)_2]_2[HOPO_3]_2$ refined as twin with 110/0-10/001 matrix and BASF=0.53.
[b] Refined from X-ray powder diffraction pattern with LaB_6 as internal standard using the program WinCSD [5].

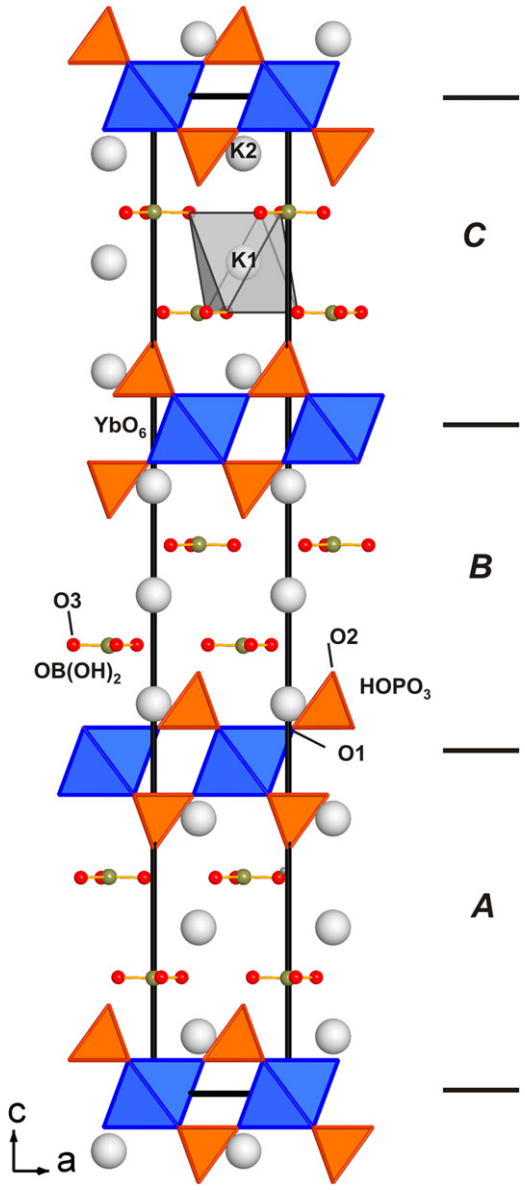

Fig. 1. Crystal structure of $K_3Yb[OB(OH)_2]_2[HOPO_3]_2$ viewed along [0 1 0]. Glaserite-type slabs are represented as YbO_6 octahedra (blue) sharing common corners with $HOPO_3$ tetrahedra (orange). White, red, and green spheres represent K-, O-, and B-atoms, respectively. The unit cell is shown as a black frame. (For interpretation of the references to color in this figure legend, the reader is referred to the web version of this article.)

Table 3
Selected interatomic distances (Å) for $K_3Yb[OB(OH)_2]_2[HOPO_3]_2$.

Atom 1	*Atom 2*	*Count*	*Distance/Å*
Yb1	–O1	6 ×	2.202(2)
P1	–O1	3 ×	1.530(2)
	–O2	1 ×	1.551(4)
K1	–O3	6 ×	2.735(2)
K2	–O1	3 ×	2.968(3)
	–O1	3 ×	2.986(2)
	–O3	3 ×	2.968(3)
B1	–O3	3 ×	1.370(2)

of 2.625(4) Å in the title compound clearly indicate the presence of protons in the crystal structure (Fig. 2). Therefore, the chemical composition "$K_3Yb[BO_3]_2[PO_4]_2^{3-}$" as determined by X-ray single-

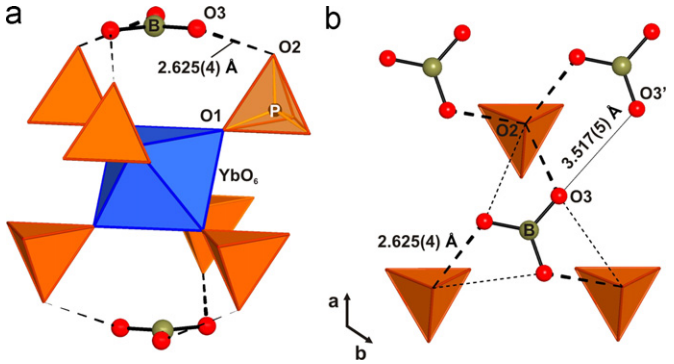

Fig. 2. Cut-out of the crystal structure of $K_3Yb[OB(OH)_2]_2[HOPO_3]_2$ showing (a) the attachment of two $OB(OH)_2$ units to a Glaserite-type slab (d(P–O2)=1.551(4) Å) and (b) two neighboring hydrogen phosphate and dihydrogen borate layers with labeled O···O distances (—: possible O–H···O bridges). For further details see text.

crystal diffraction data has been completed to $K_3Yb[OB(OH)_2]_2[HOPO_3]_2$ in order to keep the whole crystal structure neutral and avoid layers of neutral $B(OH)_3$ molecules. Boron adopts a three-fold planar coordination with oxygen (O3) at equal distances of 1.370(2) Å similar to reported values for the two polymorphs of boric acid [10]. The shortest O···O distance between the $OB(OH)_2$ units in the dihydrogen borate layer of the title compound is d(O3···O3′)=3.517(5) Å, (Fig. 2(b)), indicating only a weak hydrogen bonding interaction. In contrast, the shortest intermolecular O···O distance in layers of boric acid has been reported in the literature as d(O···O)=2.71 Å [10].

Potassium is located on two different crystallographic sites. The first coordination sphere around K1 is made up by six oxygen atoms from neighboring $OB(OH)_2$ units forming an octahedron (d(K1–O3)=2.735(2) Å, Fig. 1). Nine oxygen atoms are surrounding the K2 position with distances K2–O ranging from 2.968(2) to 2.986(3) Å. The resulting coordination polyhedron can be described as a bisected cuboctahedron with a triangle of O3 atoms as the base and a hexagon of O1 atoms on the opposite side. $OB(OH)_2$ units and $HOPO_3$ tetrahedra are separated from each other by potassium layers. According to these experimental observations, the title compound should be classified as a borate-phosphate [1].

As a consequence of the *R*-centered crystal lattice, the overall crystal structure can be rationalized by dividing it into slabs, which are stacked along [0 0 1] with the sequence …*ABC*… (Fig. 1). The Glaserite-type slabs are coordinated at their borders by $OB(OH)_2$ units together with K^+-ions in between. The attachment of the $OB(OH)_2$ groups to the Glaserite-type slabs is assumed to take place via hydrogen bonds (see O···O distances) as schematically shown in Fig. 2.

The structural elements of the title compound known from pure phosphates as well as from pure borates are combined as an intergrowth structure. This new structure type is a remarkable layered member of the small group of borate-phosphates [1]. So far, crystal structures with isolated borate and phosphate units were only reported for $M^{II}_3[BO_3][PO_4]$ (M^{II}=Mg [11,12], Co [13], Zn [12,14]), $Ln_7O_6[BO_3][PO_4]_2$ (Ln=La, Pr, Nd, Sm, Gd, Dy) [2], and the mineral Seamanite, $Mn_3(OH)_2[B(OH)_4][PO_4]$ [15]. The number of crystal structures containing isolated planar $OB(OH)_2$ units is rather low [16–19]. The first crystal structure determination was reported for $Cu_2(OH)_3[OB(OH)_2]$ [16], a compound which later on was also found to exist as a mineral (Jacquesdietrichite) [20]. Interestingly, the single-crystal structure determination using a natural mineral crystal of the Cu-phase revealed a longer B–O distance to the non-protonated oxygen (1.38(2) Å), which is in contradiction to the previous structure determination [16] and

other crystal structures, e.g. $(NEt_4)_2[OB(OH)_2]_2 \cdot B(OH)_3 \cdot 5H_2O$ [17] and $(NMe_4)[OB(OH)_2] \cdot 2(NH_2)_2CO \cdot H_2O$ [18].

In the title compound, $K_3Yb[OB(OH)_2]_2[HOPO_3]_2$, only one averaged B–O value of 1.370(2) Å is observed due to the higher crystallographic site symmetry of the dihydrogen borate ion.

3.2. Magnetic properties: magnetic susceptibility and EPR spectroscopy

The development of χ^*T with temperature change for $K_3Yb[O-B(OH)_2]_2[HOPO_3]_2$ is shown in Fig. 3(a). A slow and continuous decrease down to 1.8 K is observed. In the temperature range from 120 to 400 K a modified Curie–Weiss law ($\chi = C/(T-\theta) + \chi_0$) yields a Curie constant $C = 2.76$ emu K/mol ($\chi_0 = 0.00031$ cm^3/mol), which corresponds to an effective magnetic moment of $\mu_{eff} = 4.7\ \mu_B$ close to the expected free-ion moment of 4.54 μ_B for Yb^{3+}. The Curie–Weiss temperature of $-65(1)$ K indicates a crystal electric field interaction [21]. A magnetization isotherm (Fig. 3(b)) at 1.8 K also indicates no magnetic ordering and shows a saturation of the paramagnetic magnetization at $\approx$ 1.9 μ_B for fields above 40 kOe. However, from a low-field low-temperature Curie–Weiss fit it might be expected that ordering appears only at temperatures in the order of 0.1 K (distance $d(Yb \cdots Yb) = 5.68$ Å). Similar findings for the temperature dependent behavior of the magnetic susceptibility were reported for other Yb-containing inorganic compounds for instance $Yb(IO_3)_3$ [22] and $Cu_3Yb_3(TeO_3)_4Cl_6$ [23].

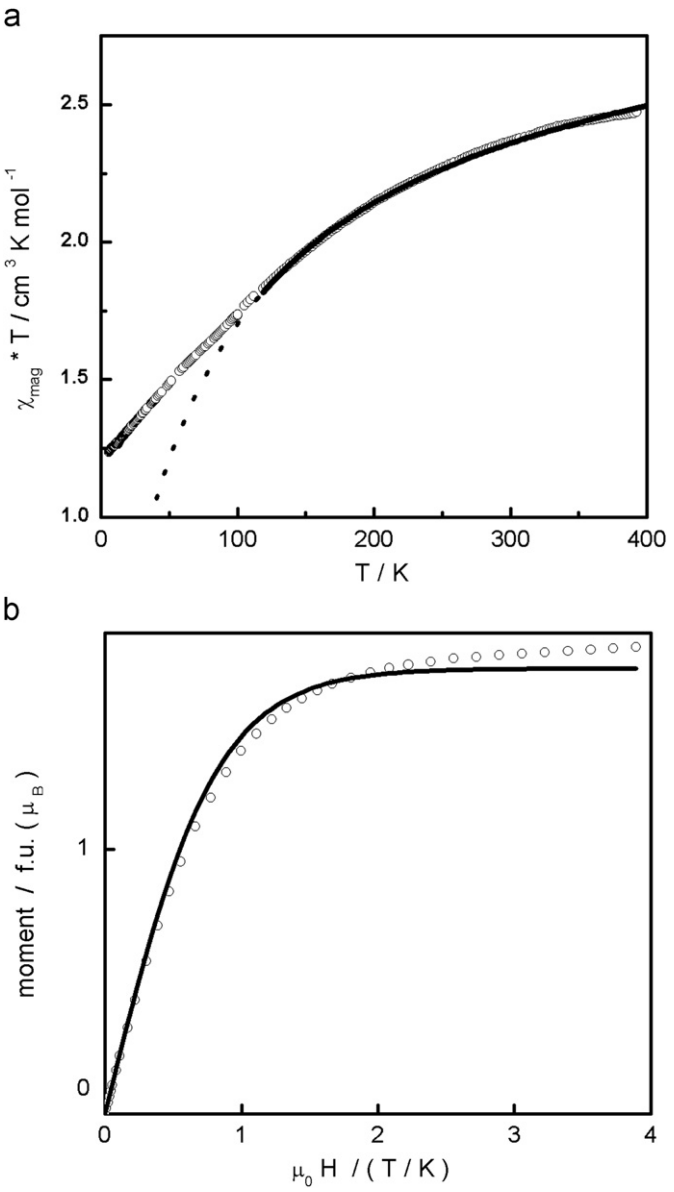

Fig. 3. Temperature and magnetic field dependence of the molar magnetic susceptibility of $K_3Yb[OB(OH)_2]_2[HOPO_3]_2$: (a) Development of χ^*T (open circles) with increase of temperature at $H_{ext} = 2000$ Oe. Curie–Weiss fit (black line) between 120 and 400 K with C = 2.76(2) emu K/mol, $\theta = -65(1)$ K, and $\chi_0 = 0.00031$ cm^3/mol. (b) The magnetization moment at 1.8 K at different magnetic fields. The solid black line represents a Brillouin function fit with fixed $J' = 1/2$ resulting in $g_{eff} = 3.71(2)$.

The continuous wave X-band (9.4 GHz) electron paramagnetic resonance (EPR) spectrum of powdered $K_3Yb[OB(OH)_2]_2[HOPO_3]_2$ is shown for $T = 5$ K in Fig. 4. A broad microwave absorption line ($\Delta H_{pp} = 830$ G) centered around 2200 G is observed. The main contribution of this line originates from five ytterbium isotopes (natural abundance 69.6%) without nuclear spin. The isotopes ^{171}Yb ($I = 1/2$) and ^{173}Yb ($I = 5/2$) show a hyperfine interaction, which leads to a broadening of the absorption line [24] and may cause the small feature at 950 G. A rough description by a single Lorentzian-type lineshape results in a g-value of 3.0(2) ($J' = 1/2$) and a linewidth of 580 G. The g-value considerably deviates from 2.6667 expected for a regular octahedral coordination. This is in agreement with the result from the single-crystal structure determination, where Yb occupies a crystal site with C_{3i} symmetry. Further support for a distorted octahedral surrounding of Yb^{3+} ions is given by the asymmetry of the central absorption line.

3.3. FT-IR spectroscopy

The IR spectrum of $K_3Yb[OB(OH)_2]_2[HOPO_3]_2$ with natural boron isotope ratio is shown in Fig. 5(a) in comparison with ^{11}B enriched $K_3Yb[OB(OH)_2]_2[HOPO_3]_2$ (Fig. 5(b)). The spectral range is divided into five characteristic regions, which will be discussed in the following section.

Absorption bands appearing in region A clearly indicate the presence of OH groups. This is in agreement with the results from thermal analysis (see below) and charge balance considerations given in Section 3.1. Similar to pure boric acid [25] four maxima are observed in region A. They originate from OH groups involved in hydrogen bonding [26]. Also hydrogen phosphates show absorption bands in this region. Therefore, an assignment to either (B)–OH or (P)–OH is not possible. Quantum chemical calculations on isolated $[OB(OH)_2]^-$ [27] obtained a shorter distance of 1.3 Å

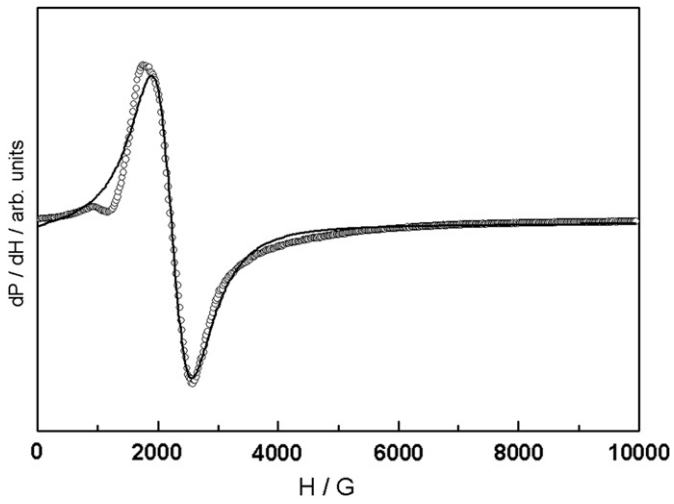

Fig. 4. Derivative (open circles) of the X-band (9.4 GHz) EPR signal for polycrystalline $K_3Yb[OB(OH)_2]_2[HOPO_3]_2$ recorded at 5 K. A fit with a single Lorentzian (black line) with a linewidth of $\Delta H = 580$ G yielded a resonance field of 2225 G, which corresponds to $g = 3.0(2)$.

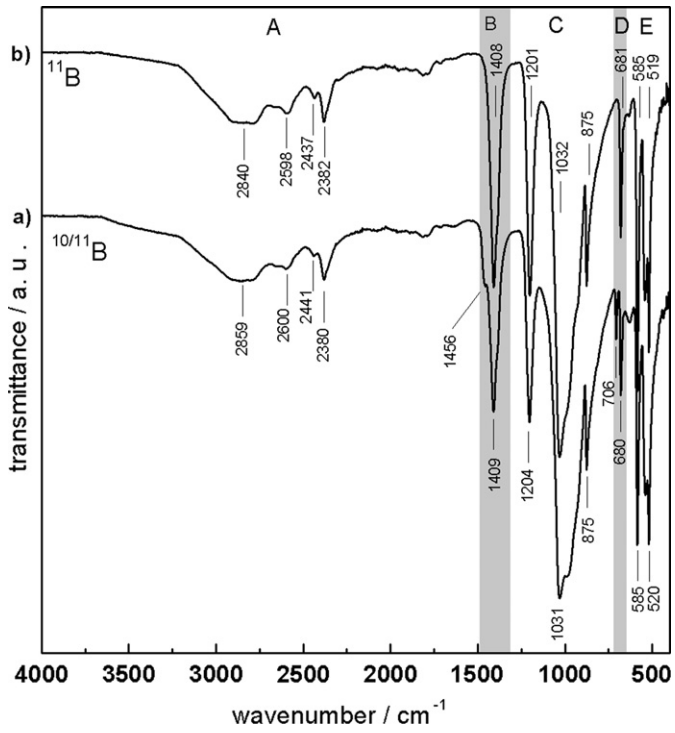

Fig. 5. FT-IR spectra (ATR) of $K_3Yb[OB(OH)_2]_2[HOPO_3]_2$: (a) with natural boron isotope ratio and with (b) ^{11}B enrichment. The different absorption regions are labeled A–E and are discussed in the text. The absorption bands marked in gray show a strong isotope effect.

between the boron atom and the non-hydrogen bonded oxygen atom, which is close to the experimental value for the well-characterized $[BO_2]^-$ anion. However, the calculated frequency of the symmetric ^{11}B–^{16}O stretching vibration appears at 1528 cm^{-1} [28], which is much lower than that for $[BO_2]^-$. This is compatible with the recorded IR spectrum of $Cu_2(OH)_3[OB(OH)_2]$ [16].

In contrast to the other regions of the spectrum the bands in region B and D show a strong isotope effect. The same was observed for matrix isolated boric acid [29]. Elaborate isotope labeling experiments together with normal mode analysis [29] led to the conclusion that the band at 1409 cm^{-1} can be assigned to a ^{11}B–O antisymmetric stretching mode and the band at 680 cm^{-1} to an out-of-plane BO_3 bending mode.

The broad structured band in region C centered around 1031 cm^{-1} can be attributed to tetrahedral phosphate anions [30]. The two well-resolved bands at 1204 and 875 cm^{-1} seen here were also observed for boric acid [25] and were assigned to an antisymmetric B–O–H bending mode and a symmetric B–O stretching mode [31]. Alternatively, these two bands may also be assigned to HPO_4^-, which similarly should appear left (P–O–H in-plane bending mode) and right (symmetric stretching mode P–O(H)) from the broad band at 1031 cm^{-1} [32].

The results from vibrational spectroscopy are in agreement with the structural model derived from single-crystal X-ray diffraction data but a conclusive decision concerning the location of the hydrogen atoms could not be made.

3.4. Thermal stability

The simultaneously recorded TG and DTA curves of $K_3Yb[OB(OH)_2]_2[HOPO_3]_2$ are shown in Fig. 6. A steep step of 7.86 wt% is observed, which is finished at about 770 K. The highest rate of mass loss coincides with an endothermic peak in the DTA trace. The total weight loss of 8.63 wt% is in agreement with the calculated value assuming a loss of 3 moles of water per formula unit (calc. 8.94 wt%). The decomposition products were identified by PXRD (Fig. S3) as $YbPO_4$ [33] and monoclinic $K_3Yb(PO_4)_2$ [34]. Profile fitting [35] yielded unit cell volumes of 277.2(1) and 384.6(1) Å^3, respectively, close to the reported values. No other crystalline compounds were found, which may indicate the presence of amorphous boron-containing components. Supporting TG-MS measurements gave no hint for a substantial evaporation of boron-containing species e.g. H_3BO_3 [36] in the investigated temperature range. Similar results were obtained for $K_3Lu[OB(OH)_2]_2[HOPO_3]_2$ (Fig. S4). The PXRD pattern can be completely fitted with the unit cell parameters for $LuPO_4$ [37] and $K_3Yb(PO_4)_2$ [8].

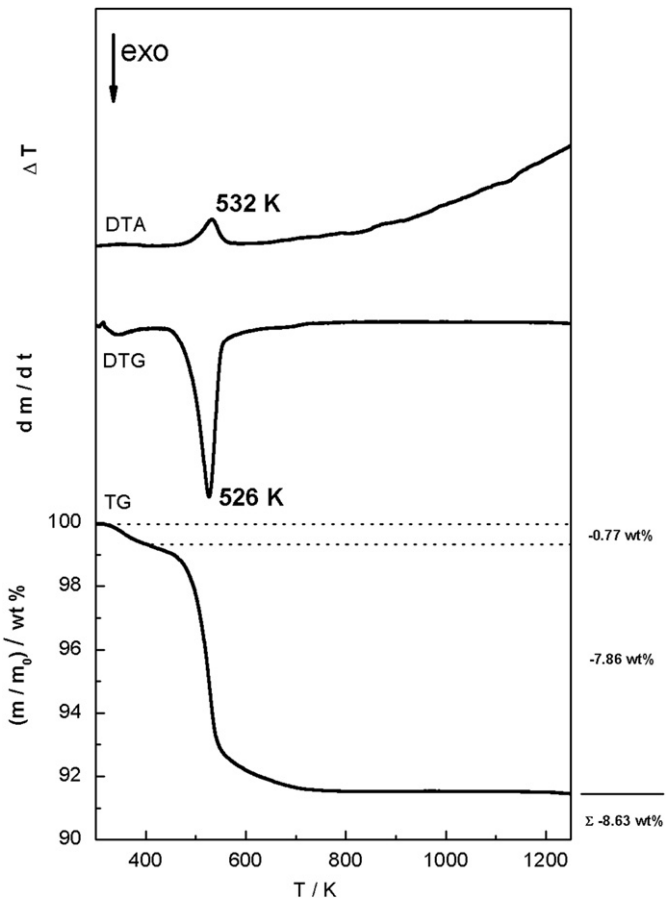

Fig. 6. DTA, TG and DTG curves of the thermal decomposition of $K_3Yb[OB(OH)_2]_2[HOPO_3]_2$ (heating rate: 5 K/min; atmosphere: argon): Between 420 and 620 K a pronounced weight loss is observed. The total weight loss of 8.63 wt % is close to the expected mass loss of 3 moles of water per formula unit (calc. 8.94 wt%).

4. Conclusion

Summarizing our results, we have shown that mild hydrothermal conditions are suitable to obtain rare-earth borate phosphates. The distinct layered character of the intergrowth structure implies the existence of even other stacking variants, the possibility of ion exchange activities and the mobility of protons, respectively.

Acknowledgment

We are indebted to Dr. G. Auffermann and A. Völzke for elemental analyses and P. Marasas for thermal analyses. Y. Zhou gratefully acknowledges financial support from the China Scholarship Council (CSC), and the National Natural Science

Foundation of China (No. 40972035). We thank Prof. C. W. Mak (University of Hong Kong), Dr. M. Wiebcke (University Hannover), Prof. T. E. Albrecht-Schmitt (University of Notre Dame), and especially Prof. A. V. Nicolaides (University of Cyprus) for the discussion on the $OB(OH)_2$ unit. We thank Dr. D. Kasinathan for proof reading the manuscript.

Appendix A. Supplementary Information

The online version of the article contains additional supplementary data, including crystallographic data of $K_3Ln[OB(OH)_2]_2[HOPO_3]_2$ (Ln = Yb, Lu), list of bond distances, PXRD and SEM pictures of $K_3Yb[OB(OH)_2]_2[HOPO_3]_2$. Supplementary data associated with this article can be found in the online version at doi:10.1016/j.jssc.2011.04.023.

References

[1] B. Ewald, Y.-X. Huang, R. Kniep, Z. Anorg. Allg. Chem. 633 (2007) 1517.
[2] (a) K.K. Palkina, S.I. Maksimova, N.T. Chibiskova, B.F. Dzhurinskii, L.Z. Gokham, Izv. Akad. Neorg. Mater. 20 (1984) 1063;
(b) Y. Shi, J.K. Liang, H. Zhang, J.L. Yang, W.D. Wang, J. Solid State Chem. 129 (1997) 45;
(c) B. Ewald, Yu. Prots, R. Kniep, Z. Kristallogr.—New. Cryst. Struct. 219 (2004) 213.
[3] G.M. Sheldrick, Acta Crystallogr. Sect. A: Found. Crystallogr. 64 (2008) 112.
[4] L.J. Farrugia, J. Appl. Cryst. 32 (1999) 837.
[5] L.G. Akselrud, P.Y. Zavalii, Y. Grin, V.K. Pecharsky, B. Baumgartner, E. Woelfel, Mater. Sci. Forum 133-136 (1993) 335.
[6] (a) B. Gossner, Neues Jb. Geologie Palaeontologie Beilage 57 (1928) 89;
(b) K. Okada, J. Ossaka, Acta Crystallogr. Sect. B: Struct. Sci. 36 (1980) 919.
[7] M. Vlasse, C. Parent, R. Salmon, G. Le Flem, P. Hagenmuller, J. Solid State Chem. 35 (1980) 318.
[8] V.A. Efremov, P.P. Melnikov, L.N. Komissarova, Koord. Khim. 38 (1981) 467.
[9] W.H. Baur, Acta Crystallogr. Sect. B: Struct. Sci. 30 (1974) 1195.
[10] (a) W.H. Zachariasen, Acta Crystallogr. 7 (1954) 305;
(b) R.R. Shuvalov, P.C. Burns, Acta Crystallogr. Sect. C: Cryst. Struct. Commun. 59 (2003) i47–i49.
[11] G. Gözel, A. Baykal, M. Kizilyalli, R. Kniep, J. Eur. Ceram. Soc. 18 (1998) 2241.
[12] J. Liebertz, S. Stähr, Z. Kristallogr. 160 (1982) 135.
[13] A. Yilmaz, X. Bu, M. Kizilyalli, R. Kniep, G.D. Stucky, J. Solid State Chem. 156 (2001) 281.
[14] K. Bluhm, C.H. Park, Z. Naturforsch. B: Chem. Sci. 52 (1997) 102.
[15] P.B. Moore, S. Ghose, Am. Mineral. 56 (1971) 1527.
[16] H. Behm, C. Baerlocher, Acta Crystallogr. Sect. C: Cryst. Struct. Commun. 41 (1985) 5.
[17] C.C. Freyhardt, M. Wiebcke, J. Chem. Soc. Chem. Commun. (1994) 1675.
[18] Q. Li, F. Xue, T.C.W. Mak, Inorg. Chem. 38 (1999) 4142.
[19] S.A. Wang, E.V. Alekseev, D.W. Juan, W.H. Casey, B.L. Phillips, W. Depmeier, T.E. Albrecht-Schmitt, Angew. Chem. Int. Ed. Engl. 49 (2010) 1057.
[20] A.R. Kampf, G. Favreau, Eur. J. Mineral. 16 (2004) 361.
[21] D. Bisui, K.N. Chattopadhyay, P.K. Chakrabarti, J. Phys. Chem. Solids 70 (2009) 59.
[22] R.E. Sykora, P. Khalifah, Z. Assefa, T.E. Albrecht-Schmitt, R.G. Haire, J. Solid State Chem. 181 (2008) 1867.
[23] D. Zhang, M. Johnsson, R.K. Kremer, Solid State Sci. 12 (2010) 536.
[24] S.K. Misra, S. Isber, Phys. B—Condens. Matter 253 (1998) 111.
[25] R.R. Servoss, H.M. Clark, J. Chem. Phys. 26 (1957) 1175.
[26] J. Dreyer, J. Chem. Phys. 122 (2005).
[27] D. Stefani, I. Pashalidis, A.V. Nicolaides, J. Mol. Struct. Theochem. 853 (2008) 33.
[28] Private communication, A.V. Nicolaides (University of Cyprus).
[29] J.S. Ogden, N.A. Young, J. Chem. Soc. Dalton Trans. (1988) 1645.
[30] A. Rulmont, R. Cahay, M. Liegeois-Duyckaerts, P. Tarte, Eur. J. Solid State Inorg. Chem. 28 (1991) 207.
[31] L. Andrews, T.R. Burkholder, J. Chem. Phys. 97 (1992) 7203.
[32] L.B. Taher, S. Chabchoub, L. Smiri-Dogguy, Solid State Sci. 1 (1999) 15.
[33] W.O. Milligan, D.F. Mullica, G.W. Beall, L.A. Boatner, Acta Crystallogr. Sect. C: Cryst. Struct. Commun. 39 (1983) 23.
[34] J. Farmer, L.A. Boatner, B.C. Chakoumakos, C.J. Rawn, J.W. Richardson, S. Khalid, Acta Crystallogr. Sect. B: Struct. Sci. 58 (2002) C138.
[35] V. Petricek, M. Dusek, L. Palatinus. Jana2006 - The crystallographic computing system. Institute of Physics, Praha, Czech Republic, 2006.
[36] M. Attina, F. Cacace, G. Occhiucci, A. Ricci, Inorg. Chem. 31 (1992) 3114.
[37] W.O. Milligan, D.F. Mullica, G.W. Beall, L.A. Boatner, Inorg. Chim. Acta 60 (1982) 39.